# Narrow Wall Axial-Slot-Coupled T Junction Between Rectangular and Circular Waveguides

B. N. DAS, P. V. D. SOMASEKHAR RAO, AND AJOY CHAKRABORTY

*Abstract*—**This paper presents an analysis of a T junction between rectangular and circular waveguides coupled through a long axial slot in the narrow wall of the rectangular waveguide. A moment method with entire orthogonal basis functions is used for deriving the expressions of the elements of the scattering matrix. The effect of the wall thickness is taken into account by treating the coupling slot as a short section of a rectangular waveguide and matching the boundary conditions at the interfaces. The conditions satisfied by the scattering matrix of the junction are verified. A comparison between the theoretical and experimental results on variation of coupling with frequency is presented.**

## I. Introduction

INVESTIGATIONS on T junctions between rectangular waveguides coupled through a rectangular slot in the feed waveguide have been reported in the literature [1]–[4]. Equivalent networks of symmetrical *H*-plane and *E*-plane T junctions of rectangular and circular waveguides coupled by a small elliptical/circular aperture in the narrow wall of the rectangular waveguide were presented by Marcuvitz [5], assuming zero wall thickness and using an integral equation approach. It would therefore be of interest to solve the problem of long slot coupling for a T junction between rectangular and circular waveguides in which the T arm is the circular waveguide.

In the present paper, a moment method analysis with entire basis functions which takes into account the effect of finite waveguide wall thickness and higher order mode coupling within the slot in the narrow wall of the rectangular waveguide is used to determine the electric field distribution in the slot aperture [6].

The coupling slot is regarded as a short section of a rectangular waveguide. The electric fields at the two interfaces of this waveguide section are determined from the boundary conditions and the relations between the incident and reflected waves at the two interfaces. From a knowledge of the electric field distribution at the two interfaces, the amplitude and the phase of the reflected and coupled waves are found.

The problem is formulated for the cases where the signal is fed to one of the arms of the rectangular guide and to the circular guide, the other ports being assumed match terminated in both cases. The variation of coupling with frequency for a particular slot length is evaluated for both cases, and a comparison with the experimental data is presented.

From the results of the analysis, the scattering matrix of the junction is found, and the conditions satisfied by the scattering matrix of such a junction of dissimilar waveguides are verified. This is believed to be the first evaluation of the scattering matrix parameters of this type of junction using the moment method analysis.

Manuscript received September 19, 1988; revised February 28, 1989.

The authors are with the Department of Electronics and Electrical Communication Engineering, Indian Institute of Technology, Kharagpur, 721 302 India.

IEEE Log Number 8930754

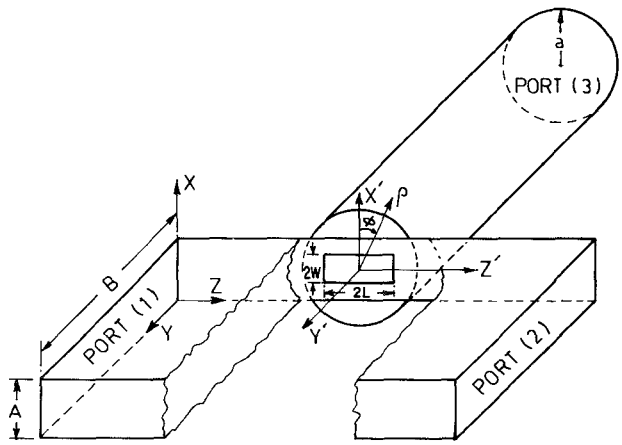


Fig. 1. T junction between rectangular and circular waveguides.

## II. Analysis

Fig 1 shows the geometry of a T junction between rectangular and circular waveguides, coupled through a long axial slot of length $2L$ and width $2W$, centered in the narrow wall of the rectangular waveguide.

A rectangular slot in the narrow wall of a waveguide of wall thickness $t$ can be regarded as a short section of a rectangular guide, as illustrated in Fig. 2 (expanded view). Since the width of the slot is very small, variation of the field along the narrow dimension of this slot waveguide is neglected. The field inside the short waveguide section ⓐ–ⓑ is therefore described as a superposition of $TE_{t0}$ modes.

Following the moment method analysis with entire basis functions as suggested by Josefsson [6], the analysis of the

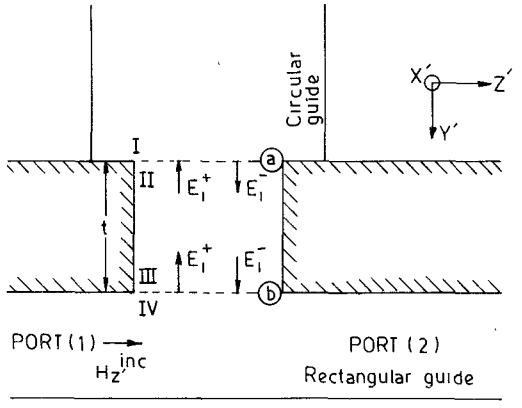


Fig. 2. Representation of the coupling slot as a section of a waveguide, coupling the rectangular and circular guides.

T junction of Fig. 1 is carried out on the basis of the boundary conditions at the interfaces ⓐ or (I/II) and ⓑ or (III/IV) of Fig. 2 for the cases when (i) the signal is fed to port (1) of the rectangular guide and (ii) the signal is fed to port (3) of the circular guide.

*A. Case (i): Signal Fed to Port (1)*

The excitation is applied to port (1) with the other ports being assumed match terminated. For an $i$th mode traveling in the waveguide section ⓐ–ⓑ toward interface ⓐ, continuity of the tangential magnetic fields at the same interface yields the following equation:

$$E_i^+ e_i Y_i - \sum_{q=1}^{N} E_q^- e_q Y_q = H_{Z'}^c(E_i^+ e_i) + H_{Z'}^c(E_q^- e_q) \quad (1)$$

where $E_i^+$ and $E_q^-$ are the amplitude coefficients, having dimensions of V/m, and the superscripts + and − indicate the directions of propagation as shown in Fig. 2. $H_{Z'}^c$ is the transverse component of the magnetic field in the circular guide, due to the electric field in the slot aperture (I/II) at interface ⓐ, and has the dimension of A/m. The basis functions $e_q$ and $e_i$ are dimensionless quantities, given by [6]

$$e_J(Z') = \sin\frac{J\pi}{2L}(Z'+L) \qquad (J=q,i) \quad (2)$$

and $Y_J$ is the modal admittance for the $TE_{J0}$ modes in the waveguide section. Further, $H_{Z'}^c$ is evaluated as a function of $E_q^- e_q$ and $E_i^+ e_i$ and is expressed in the form

$$H_{Z'}^c = E_J \xi^c(e_J) \qquad (J=q,i). \quad (3)$$

Taking the inner products of (1) with the testing functions

$$w_s = \sin\frac{s\pi}{2L}(Z'+L) \quad (4)$$

and considering the superposition of $TE_{i0}$ modes, the following matrix equation is obtained:

$$[E^-]_{II} = [Y^{cw}]^{-1}[h^{cw}][E^+]_{II}. \quad (5)$$

The elements of the square matrices on the right-hand side of (5) are of the form

$$Y_{qs}^{cw} = \langle \xi^c(e_q), w_s \rangle + Y_q 2LW\delta_{qs} \quad (6)$$

$$h_{is}^{cw} = -\langle \xi^c(e_i), w_s \rangle + Y_i 2LW\delta_{is} \quad (7)$$

and $\delta$ is the Kronecker delta.

For a dominant mode incident magnetic field $H_{Z'}^{inc}$ from port (1) and the $i$th mode excited in the waveguide section ⓐ–ⓑ, the boundary condition at the interface ⓑ is of the form

$$H_{Z'}^r(E_i^- e_i) + H_{Z'}^r(E_q^+ e_q) + H_{Z'}^{inc} = -E_i^- e_i Y_i + \sum_{q=1}^{N} E_q^+ e_q Y_q \quad (8)$$

where $H_{Z'}^r$ is the longitudinal component of the magnetic field (A/m) in the rectangular guide, due to the electric field distribution in the slot aperture (III/IV) at the interface ⓑ, and is expressed as a function of $E_q^+ e_q$ and $E_i^- e_i$ in the form

$$H_{Z'}^r = E_J \xi^r(e_J) \qquad (J=q,i). \quad (9)$$

The expression for $H_{Z'}^{inc}$ in the rectangular guide of Fig. 2 is given by [8]

$$H_{Z'}^{inc} = \frac{1}{j\omega\mu}\frac{\pi}{B}\sqrt{\frac{2}{AB}}\cos\frac{\pi Y}{B}e^{-j\beta Z'}. \quad (10)$$

Equation (10) is substituted into (8) and the inner products with the testing functions of (4) are evaluated. The full solution, obtained by taking the superposition of the incident $TE_{i0}$ modes, is of the form [6], [9]

$$[E^+]_{III} = [Y^{rw}]^{-1}\{[h^{rw}][E^-]_{III} - [h^{inc}]\} \quad (11)$$

where the elements of the column matrix $[h^{inc}]$ are

$$h_s^{inc} = \langle H_{Z'}^{inc}, w_s \rangle \quad (12)$$

and the elements of the square matrices $[Y^{rw}]$ and $[h^{rw}]$ are

$$Y_{qs}^{rw} = \langle \xi^r(e_q), w_s \rangle - Y_q 2LW\delta_{qs} \quad (13)$$

$$h_{is}^{rw} = -\langle \xi^r(e_i), w_s \rangle - Y_i 2LW\delta_{is}. \quad (14)$$

The incident and reflected waves at the two interfaces are related by the equations

$$[E^+]_{II} = [B][E^+]_{III} \quad (15)$$

and

$$[E^-]_{III} = [B][E^-]_{II} \quad (16)$$

where $[B]$ is the diagonal matrix with elements $\exp(-\gamma_{i0}t)$, $\gamma_{i0}$ being the propagation constant of the $i$th TE mode in the waveguide section ⓐ–ⓑ and $i=1,2,3,\cdots,N$. Over the frequency range of interest, 8.4 to 9.6 GHz, for a slot length of 1.690 cm, $\gamma_{20}, \gamma_{30}, \cdots, \gamma_{N0}$ are always real, and $\gamma_{10}$ is real for frequencies below 8.876 GHz only.

Combining (15), (16), (5), and (11), the total tangential electric field at interface ⓑ is obtained in the same form as given in [6, eq. (23)] (however, the individual matrix elements will be different), and is expressed as

$$[E^{b,1}] = \{[U] + [B][Y^{cw}]^{-1}[h^{cw}][B]\}[E^+]_{III} \quad (17)$$

where

$$[E^+]_{III} = \left\{[Y^{rw}]^{-1}[h^{rw}][B][Y^{cw}]^{-1}[h^{cw}][B]-[U]\right\}^{-1} \cdot [Y^{rw}]^{-1}[h^{inc}]. \quad (18)$$

$[U]$ is the unit matrix, and the superscript 1 indicates that the excitation is from port (1) of the rectangular guide.

In similar fashion, the total tangential electric field in the aperture plane of the slot at interface ⓐ is obtained by combining (15), (5), and (18) as

$$[E^{a,1}] = \left\{[B]+[Y^{cw}]^{-1}[h^{cw}][B]\right\}[E^+]_{III}. \quad (19)$$

The expressions for the elements of the different matrices appearing in (17)–(19) are derived in the following section.

*B. Expressions for Elements of the Matrices for Case (i)*

Using (10) and (4) in (12) and carrying out the integration over the slot aperture, the elements of the column matrix $[h^{inc}]$ are obtained as

$$h_s^{inc} = \frac{1}{j\omega\mu}\frac{\pi}{B}\sqrt{\frac{2}{AB}}\frac{2W(s\pi/L)}{\beta^2-(s\pi/2L)^2} \cdot \begin{bmatrix} -\cos\beta L & \text{for } s \text{ odd} \\ -j\sin\beta L & \text{for } s \text{ even} \end{bmatrix} \quad (20)$$

where

$$\beta = \frac{\pi}{B}\sqrt{\left(\frac{2B}{\lambda}\right)^2-1}. \quad (21)$$

Using (2), the relation for the $Z$-directed magnetic current in the slot aperture (III/IV) of the form

$$M_Z\bar{U}_Z = [E_J e_J(Z)\bar{U}_X]\times\bar{U}_Y \qquad (J=q,i) \quad (22)$$

and following the method suggested in the literature [10], [1], the expression for $H_Z^r(e_J)$ is derived, from which $\xi^r(e_J)$ is obtained as

$$\xi^r(e_J) = \frac{1}{j\omega\mu}\sum_n^\infty\sum_m^\infty \frac{\epsilon_n\epsilon_m}{2AB\gamma}\cos\frac{n\pi X}{A}\cos\frac{m\pi Y}{B} \cdot\left\{2W\cos\left(\frac{n\pi}{2}\right)\frac{\sin(n\pi W/A)}{n\pi W/A}\right\} \cdot\frac{1}{\gamma^2+\left(\frac{J\pi}{2L}\right)^2}\left[2\gamma\sin\left\{\frac{J\pi}{2L}(Z+L)\right\} \cdot\left\{K^2-\left(\frac{J\pi}{2L}\right)^2\right\} + (J\pi/2L)e^{-\gamma L}(K^2+\gamma^2)(e^{-\gamma Z}-e^{\gamma Z}\cos J\pi)\right] \quad (23)$$

where $\epsilon_n, \epsilon_m$ are the Neumann numbers and $\gamma = \sqrt{(n\pi/A)^2+(m\pi/B)^2-K^2}$.

Equation (23) is substituted into (13) and (14) and the matrix elements are obtained as

$$Y_{qs}^{rw} = Y_{qs}^r - Y_q 2LW\delta_{qs} \quad (24)$$

and

$$h_{is}^{rw} = -Y_{is}^r - Y_i 2LW\delta_{is} \quad (25)$$

where

$$Y_{Js}^r = \frac{1}{j\omega\mu}\frac{(2W)^2}{AB}\sum_n^\infty\sum_m^\infty\frac{\epsilon_n\epsilon_m}{2}\left\{\cos\left(\frac{n\pi}{2}\right)\frac{\sin(n\pi W/A)}{n\pi W/A}\right\}^2 \cdot\left[\frac{J\pi/2L}{\gamma^2+\left(\frac{J\pi}{2L}\right)^2}\frac{s\pi/2L}{\gamma^2+\left(\frac{s\pi}{2L}\right)^2}\frac{2(K^2+\gamma^2)}{\gamma} \cdot\begin{Bmatrix}1+e^{-2\gamma L} & \text{for } J,s \text{ odd}\\ 1-e^{-2\gamma L} & \text{for } J,s \text{ even}\end{Bmatrix} + \frac{K^2-(J\pi/2L)^2}{\gamma^2+\left(\frac{J\pi}{2L}\right)^2}2L\delta_{Js}\right] = 0 \quad \text{for } J \text{ odd, } s \text{ even and } s \text{ odd, } J \text{ even.} \quad (26)$$

Derivation of the expressions for the matrix elements using (6) and (7) demands a knowledge of the magnetic field $H_{Z'}^c$ in the transverse plane of the circular guide at interface ⓐ of Fig. 2. $H_{Z'}^c$ can be expressed in terms of the radial and circumferential components of the magnetic field in the transverse plane of the circular guide as [8]

$$H_{Z'}^c = H_\rho\sin\phi + H_\phi\cos\phi. \quad (27)$$

$H_\rho$ and $H_\phi$ can be obtained from the formula for the total transverse component $\bar{H}_t$, available in the literature [3], [4], [8]. Substituting the expression for $H_{Z'}^c$ thus obtained into (6) and (7), the elements of the square matrices $[Y^{cw}]$ and $[h^{cw}]$ are obtained as

$$Y_{qs}^{cw} = \sum_n\sum_p\left[V_{np,q}^e V_{np,s}^e Y_{np}^e + V_{np,q}^m V_{np,s}^m Y_{np}^m\right] + Y_q 2LW\delta_{qs} \quad (28)$$

$$h_{is}^{cw} = -\sum_n\sum_p\left[V_{np,i}^e V_{np,s}^e Y_{np}^e + V_{np,i}^m V_{np,s}^m Y_{np}^m\right] + Y_i 2LW\delta_{is} \quad (29)$$

where

$$V_{np,r}^e = -4\sqrt{\frac{\epsilon_n}{\pi(X_{np}'^2-n^2)}}\frac{1}{J_n(X_{np}')} \cdot\sin\left(\frac{r\pi}{2}\right)\int_{X'=0}^W\int_{Z'=0}^L\cos\left(\frac{r\pi Z'}{2L}\right) \cdot\left[\frac{n}{\rho}J_n\left(X_{np}'\frac{\rho}{a}\right)\cos(n+1)\phi + \frac{X_{np}'}{a} \cdot J_{n-1}\left(X_{np}'\frac{\rho}{a}\right)\sin n\phi\sin\phi\right]dZ'\,dX' \quad (30)$$

$$V_{np,r}^{m} = -4\sqrt{\frac{\epsilon_n}{\pi}}\frac{1}{X_{np}J_{n+1}(X_{np})} \cdot \sin\left(\frac{r\pi}{2}\right)\int_{X'=0}^{W}\int_{Z'=0}^{L}\cos\left(\frac{r\pi Z'}{2L}\right) \cdot\left[-\frac{n}{\rho}J_n\left(X_{np}\frac{\rho}{a}\right)\cos(n+1)\phi + \frac{X_{np}}{a}J_{n-1}\left(X_{np}\frac{\rho}{a}\right)\cos n\phi\cos\phi\right]dZ'\,dX' \quad (31)$$

for all $n$ odd and $r = q$, $i$, or $s$. Also

$$\rho = \sqrt{(X')^2+(Z')^2} \qquad \phi = \tan^{-1}(Z'/X')$$

$$Y_{np}^{e} = \frac{\gamma_{np}}{j\omega\mu} \qquad Y_{np}^{m} = \frac{j\omega\epsilon}{\gamma_{np}} \qquad \gamma_{np} = \sqrt{(K_c^2 - K^2)}$$

with

$$K_c(\mathrm{TE}) = \frac{X'_{np}}{a} \quad \text{and} \quad K_c(\mathrm{TM}) = \frac{X_{np}}{a}.$$

*C. Case (ii): Signal Fed to Port (3)*

Consider the T junction of Fig. 1 when the input is from the circular guide (T arm). For a dominant mode incident wave $H_{Z'}^{\mathrm{inc},3}$ in port (3) of Fig. 2, the boundary conditions at the two interfaces are

$$H_{Z'}^{r}(E_q^{+}e_q) - \sum_{q=1}^{N} E_q^{+}e_qY_q = -\left[H_{Z'}^{r}(E_i^{-}e_i) + E_i^{-}e_iY_i\right] \qquad \text{at } ⓑ \quad (32)$$

and

$$H_{Z'}^{c}(E_q^{-}e_q) + \sum_{q=1}^{N} E_q^{-}e_qY_q = -\left[H_{Z'}^{c}(E_i^{+}e_i) - E_i^{+}e_iY_i\right] - 2H_{Z'}^{inc,3} \qquad \text{at } ⓐ. \quad (33)$$

Using relation (27) and the expressions for the orthonormalized $H_\rho$ and $H_\phi$ components available in the literature for the dominant mode in the circular guide [8], the expression for $H_{Z'}^{\mathrm{inc},3}$ is obtained as

$$H_{Z'}^{\mathrm{inc},3} = \sqrt{\frac{2}{\pi(X_{11}'^2-1)}}\frac{Y_{11}^{e}}{J_1(X'_{11})}\left[\frac{X'_{11}}{a}J_1'\left(\frac{X'_{11}\rho}{a}\right)\sin^2\phi + \frac{1}{\rho}J_1\left(\frac{X'_{11}\rho}{a}\right)\cos^2\phi\right]e^{-j\beta_{11}Y'}. \quad (34)$$

The superscript 3 indicates the port of excitation, and $\beta_{11}$ and $Y_{11}^{e}$ are the phase constant and characteristic wave admittance of the dominant mode. The factor of 2 in (33) results from the in-phase reflection of the incident magnetic field at the electric wall terminating the circular guide.

Equations (32) and (33) are transformed into matrix equations by taking the inner products with testing functions of (4) and are given by

$$[E^{+}]_{\mathrm{III}} = [Y^{rw}]^{-1}[h^{rw}][E^{-}]_{\mathrm{III}} \qquad \text{at } ⓑ \quad (35)$$

and

$$[E^{-}]_{\mathrm{II}} = [Y^{cw}]^{-1}\{[h^{cw}][E^{+}]_{\mathrm{II}} - [2h^{\mathrm{inc},3}]\} \qquad \text{at } ⓐ. \quad (36)$$

The square matrices $[Y^{rw}]$, $[h^{rw}]$, $[Y^{cw}]$, and $[h^{cw}]$ appearing in (35) and (36) are given by (13), (14) and (6), (7). The elements of these square matrices are therefore obtained from (24)–(31). The elements of the column matrix $[h^{\mathrm{inc},3}]$ are, however, different.

Substituting (34) and (4) into (12), the elements of the column matrix $[h^{\mathrm{inc},3}]$ are obtained as

$$h_s^{\mathrm{inc},3} = \sqrt{\frac{2}{\pi(X_{11}'^2-1)}}\frac{4Y_{11}^{e}}{J_1(X'_{11})} \cdot \sin\left(\frac{s\pi}{2}\right)\int_{X'=0}^{W}\int_{Z'=0}^{L}\cos\left(\frac{s\pi Z'}{2L}\right) \cdot\left[\frac{1}{\rho}J_1\left(X'_{11}\frac{\rho}{a}\right) - \frac{X'_{11}}{a}J_2\left(X'_{11}\frac{\rho}{a}\right)\sin^2\phi\right]dZ'\,dX'. \quad (37)$$

Combining (35), (36) and (15), (16), the total tangential electric fields in the slot aperture at interfaces ⓐ and ⓑ are obtained as

$$[E^{a,3}] = \{[U] + [B][Y^{rw}]^{-1}[h^{rw}][B]\}[E^{-}]_{\mathrm{II}} \qquad \text{at } ⓐ \quad (38)$$

$$[E^{b,3}] = \{[B] + [Y^{rw}]^{-1}[h^{rw}][B]\}[E^{-}]_{\mathrm{II}} \qquad \text{at } ⓑ \quad (39)$$

where

$$[E^{-}]_{\mathrm{II}} = \{[Y^{cw}]^{-1}[h^{cw}][B][Y^{rw}]^{-1}[h^{rw}][B] - [U]\}^{-1} \cdot [Y^{cw}]^{-1}[2h^{\mathrm{inc},3}]. \quad (40)$$

## III. Scattering Matrix

The analysis presented above permits the evaluation of the scattering matrix parameters of the T junction of Fig. 1. For this three-port junction $S_{11} = S_{22}$, $S_{12} = S_{21}$, $S_{13} = S_{23}$, and $S_{31} = S_{32}$. Therefore, the evaluation of $S_{11}$, $S_{12}$, $S_{13}$, $S_{31}$, and $S_{33}$ is sufficient for the description of the complete $3\times3$ scattering matrix of the junction.

The $[S]$ matrix of a junction with dissimilar impedances of lines connected to the ports satisfies the following reciprocity relation [7]:

$$[Z_0^{-1}][S] = [\bar{S}][Z_0^{-1}] \quad (41)$$

where $[\bar{S}]$ is the transpose of the matrix $[S]$. For the junction of Fig. 1 the diagonal matrix $[Z_0^{-1}]$ has diagonal elements $1/Z_{01}$, $1/Z_{01}$, and $1/Z_{11}$, $Z_{01}$ and $Z_{11}$ being, respectively, the dominant mode characteristic wave impedances of the rectangular and circular waveguides.

Further, since the junction is lossless, the $[S]$ matrix also satisfies the following relation [7]:

$$[S]^{\dagger}[Z_0^{-1}][S] = [Z_0^{-1}] \tag{42}$$

where $[S]^{\dagger}$ is the complex conjugate transpose of $[S]$.

### A. Elements of the Scattering Matrix

The derivation of the expressions for the parameters $S_{11}$, $S_{12}$, $S_{31}$ of the scattering matrix demands a knowledge of the dominant mode longitudinal components of the magnetic fields $H_Z^{\text{back}}$ and $H_Z^{\text{forw}}$ traveling, respectively, towards ports (1) and (2) of the rectangular guide of Fig. 1 and a knowledge of the dominant mode modal voltage $\vartheta_{11}^e$ in the circular waveguide when the junction is excited from port (1).

Using (22) and (2), the amplitude coefficients obtained from (17) and (18), and the expressions for $F_Z$ and $H_Z$ available in the literature [1, eqs. (3) and (5)], evaluation of the integrals for $m=1$ and $n=0$ yields expressions for the dominant mode forward and backward traveling waves $H_Z^{\text{forw}}$ and $H_Z^{\text{back}}$. From these expressions, $S_{11}$ and $S_{12}$ are obtained as

$$S_{11} = H_Z^{\text{back}}/H_Z^{\text{inc}}$$

or

$$S_{11} = \sum_{q=1}^{N} E_q^{b,1} \frac{2W}{\beta} \frac{q\pi/L}{(q\pi/2L)^2-\beta^2} \frac{\pi}{B\sqrt{2AB}} \cdot \begin{cases} -j\cos\beta L & \text{for } q \text{ odd} \\ \sin\beta L & \text{for } q \text{ even} \end{cases} \tag{43}$$

and

$$S_{12} = \left(H_Z^{\text{inc}} + H_Z^{\text{forw}}\right)/H_Z^{\text{inc}}$$

or

$$S_{12} = 1 + \sum_{q=1}^{N} E_q^{b,1} \frac{2W}{\beta} \frac{q\pi/L}{(q\pi/2L)^2-\beta^2} \frac{\pi}{B\sqrt{2AB}} \cdot \begin{cases} -j\cos\beta L & \text{for } q \text{ odd} \\ -\sin\beta L & \text{for } q \text{ even} \end{cases}. \tag{44}$$

For the incident field given by (10), the modal voltage is unity. Hence, the matrix element $S_{31}$ is defined as

$$S_{31} = \vartheta_{11}^e = \sum_{q=1}^{N} E_q^{a,1} V_{11,q}^e \tag{45}$$

and $V_{11,q}^e$ is obtained from (30) by substituting $n=1$ and $p=1$.

The matrix elements $S_{33}$ and $S_{13}$ are evaluated from a knowledge of the modal voltages of the incident and reflected waves in the circular guide and of the dominant mode modal voltage $\vartheta_{01}^e$ of the wave coupled into port (1) of the rectangular guide, when the excitation is applied to port (3).

For an orthonormalized dominant mode incident field of the form given in (34), the modal voltage is unity [8]. Therefore, $S_{33}$ and $S_{13}$ are expressed as

$$S_{33} = -1 + \vartheta_{11}^e = -1 + \sum_{q=1}^{N} E_q^{a,3} V_{11,q}^e \tag{46}$$

$$S_{13} = \vartheta_{01}^e \tag{47}$$

where $\vartheta_{11}^e$ is the modal voltage of the scattered wave in the circular guide due to the electric field distribution in the slot aperture ⓐ, and $V_{11,q}^e$ is obtained from (30).

Determination of $\vartheta_{01}^e$ appearing in (47) involves derivation of an expression for the magnetic field traveling into port (1), which is found using (22), (2), the amplitude coefficients obtained from (39) and (40), and (3) and (5) of [1]. The corresponding electric field in the rectangular guide is obtained from the relations between $E$ and $H$ [11], from which the modal voltage $\vartheta_{01}^e$ is determined [8]. The resulting expression for $S_{13}$ is of the form

$$S_{13} = \sum_{q=1}^{N} E_q^{b,3} \frac{\pi}{B} \sqrt{\frac{AB}{2}} \frac{2W}{AB\beta} \frac{q\pi/L}{(q\pi/2L)^2-\beta^2} \cdot \begin{cases} -j\cos\beta L & \text{for } q \text{ odd} \\ \sin\beta L & \text{for } q \text{ even} \end{cases}. \tag{48}$$

### B. Estimation of Coupling

When the junction is excited from port (1) of the rectangular guide, the expressions for the incident and coupled powers are of the form

$$P_{\text{in}} = 1/Z_{01} \tag{49}$$

and

$$P_{\text{coup}} = |\vartheta_{11}^e|^2/Z_{11}. \tag{50}$$

Therefore, the coupling, for the case of excitation from port (1), is given by

$$C_1 = 10\log\left(\frac{P_{\text{coup}}}{P_{\text{in}}}\right) = 10\log\left[\frac{|\vartheta_{11}^e|^2}{Z_{11}} Z_{01}\right] \quad \text{dB}. \tag{51}$$

When the excitation is applied to port (3), the expression for coupling is similarly obtained as

$$C_3 = 10\log\left[\frac{|\vartheta_{01}^e|^2}{Z_{01}} Z_{11}\right] \quad \text{dB}. \tag{52}$$

## IV. Numerical and Experimental Results

For the structure shown in Fig. 1, using (20) and (21), (24)–(31), (17)–(19), and (37)–(40), the complex amplitude coefficients are evaluated over the frequency range 8.4 to 9.6 GHz, at the interfaces ⓐ and ⓑ, for a rectangular coupling slot of dimensions $2L=1.690$ cm, $2W=0.107$ cm, and waveguide dimensions $A=1.016$ cm, $B=2.286$ cm, $t$ (wall thickness) $=0.127$ cm, and $a=1.185$ cm. The integrations in (30) and (31) are numerically evaluated using Gaussian quadrature. The computations are carried out for the basis functions $N=1$, 3, and 5.

From a knowledge of the computed complex amplitude coefficients, the parameters $S_{11}$, $S_{12}$, $S_{31}$, $S_{13}$, and $S_{33}$ are evaluated using (43)–(45), (48), and (46). The numerical data on $S_{11}$, $S_{12}$, $S_{31}$ are presented in Fig. 3, and those on $S_{13}$ and $S_{33}$ are presented in Fig. 4 as a function of frequency.

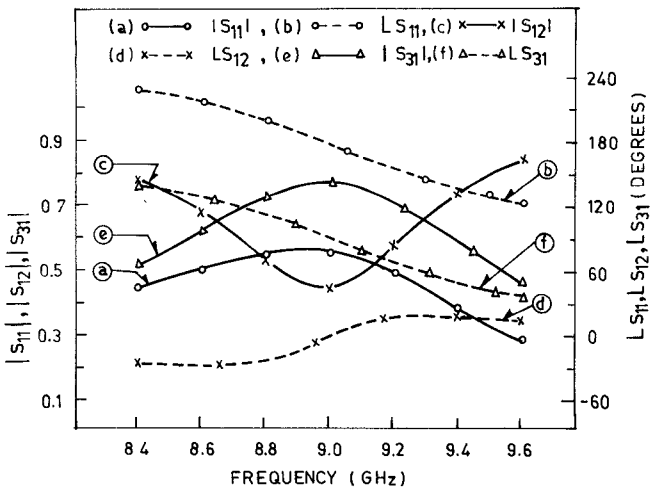


Fig. 3. Variation of magnitude and phase of $S_{11}$, $S_{12}$ and $S_{31}$ with frequency (theoretical): (a) $|S_{11}|$, (b) $\angle S_{11}$, (c) $|S_{12}|$, (d) $\angle S_{12}$, (e) $|S_{31}|$, (f) $\angle S_{31}$.

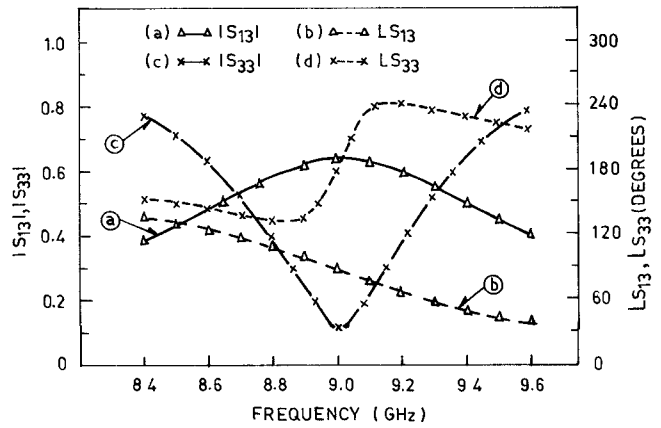


Fig. 4. Variation of magnitude and phase of $S_{13}$ and $S_{33}$ with frequency (theoretical): (a) $|S_{13}|$, (b) $\angle S_{13}$, (c) $|S_{33}|$, (d) $\angle S_{33}$.

Using the numerical values of the elements of the $S$ matrix, relations (41) and (42) for the T junction of dissimilar waveguides are verified over the frequency range 8.4 to 9.6 GHz. Carrying out matrix multiplication on the left-hand side of (42), it is found that the elements of the principal diagonal of the resulting matrix are exactly equal to $1/Z_{01}$, $1/Z_{01}$, and $1/Z_{11}$ over the above frequency range and that the nondiagonal elements are negligibly small. These results justify the validity of the analysis presented above.

Using (51), (52), (45), (30), (47), and (48), the variations of $C_1$ and $C_3$ are evaluated for the above slot parameters and waveguide dimensions over the frequency range 8.4 to 9.6 GHz. The two results are found to be exactly identical. It is found that there is no significant change in the variation of coupling for $N = 3$ and $N = 5$. The computed results are therefore presented for $N = 5$ in Fig. 5. In the same figure, the variation of coupling with frequency is also presented for the zero-thickness case ($t = 0$) for $N = 5$.

For the sake of comparison, the experimental data, obtained using a Hewlett Packard frequency response test set (type 182 T) and dual directional coupler (type 11692 D), are also presented in Fig. 5. The coupling has been measured when the signal is fed to port (1) as well as when the signal is fed to port (3). The two experimental results differ by about 0.1 to 0.2 dB over the above frequency range of interest.

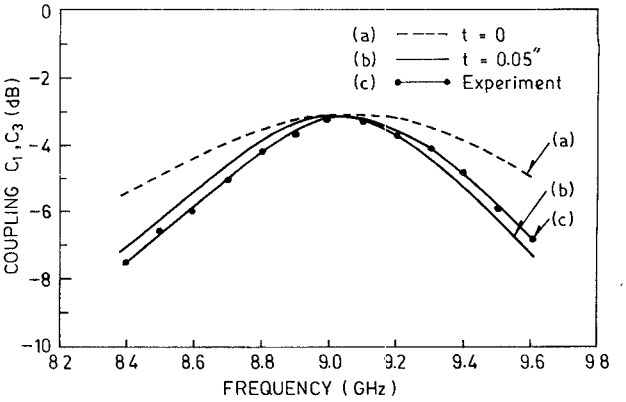


Fig. 5. Variation of coupling with frequency: (a) $t = 0$ (theoretical), (b) $t = 0.05$ in. (theoretical), (c) experimental.

## V. Discussion

Application of the moment method for investigating the waveguide junction problem of composite coordinate systems permits evaluation of the complex scattering matrix of the junction. The other methods suggested in the literature [1]–[4] have not been found convenient for the evaluation of the complete $S$ matrix of the junction.

From a knowledge of the scattering parameters, it is possible to calculate the coupled power and the complex reflection coefficient for any termination of the ports of the junction. The numerical and experimental results are, however, presented for matched termination of the different ports.

Using the diagonal elements of the scattering matrix, it is possible to determine the admittance seen by the generator at the intersection of the planes of symmetry of the junction. It is worthwhile to point out that this admittance is complex, and the frequency for zero susceptance, called the resonant frequency, changes by about 40 MHz for a change in slot length of 0.01 cm.

Analysis by the method of moments also permits a determination of the exact field distribution in the aperture plane of the coupling slot. It is found that the amplitude coefficients resulting in odd field distribution in the slot aperture become zero when the excitation is applied to port (3). For excitation from the other ports, however, all the coefficients have nonzero values; therefore the corresponding electric field in the slot aperture does not have a purely symmetric distribution.

For the particular circular waveguide chosen for computation and experimentation, the cutoff frequency for the next higher order mode is 9.69 GHz. The results are therefore presented up to a maximum frequency of 9.6 GHz.

The numerical results on the $S$ matrix satisfy the reciprocity and losslessness condition for the three-port network terminated in lines of unequal wave impedances. It is worthwhile to point out that the losslessness condition corresponds to the unitary property of the $S$ matrix when line impedances are identical. Verification of the conditions mentioned above justifies the validity of the analysis.

There is a good agreement between the theoretical and experimental results of coupling when the effect of finite wall thickness is taken into account. The theoretical results for zero wall thickness show a considerable deviation from those for finite wall thickness.

## References


[1] V. M. Pandharipande and B. N. Das, "Equivalent circuit of a narrow wall waveguide slot coupler," *IEEE Trans. Microwave Theory Tech.*, vol. MTT-27, pp. 800–804, 1979.

[2] B. N. Das, P. S. Deshmukh, and V. M. Pandharipande, "Excitation of planar slot array from rectangular waveguide," *Proc. Inst. Elec. Eng.*, vol. 131, pt. H, pp. 99–101, 1984.

[3] B. N. Das, G. S. N. Raju, and A. Chakraborty, "Investigations on a new type of inclined-slot coupled T-junction," *Proc. Inst. Elec. Eng.*, vol. 134, pt. H, pp. 473–476, 1987.

[4] ____, "Analysis of coplanar $E-H$ plane T-junction using dissimilar rectangular waveguides," *IEEE Trans. Microwave Theory Tech.*, vol. 36, pp. 604–606, Mar. 1988.

[5] N. Marcuvitz, *Waveguide Handbook*. New York: Dover, 1965.

[6] L. G. Josefsson, "Analysis of longitudinal slots in rectangular waveguides," *IEEE Trans. Antennas Propagat.*, vol. AP-35, pp. 1351–1357, Dec. 1987.

[7] D. M. Kerns, "Plane wave scattering matrix theory of antennas and antenna–antenna interactions," NBS Monograph 162, June 1981.

[8] R. F. Harrington, *Time-Harmonic Electromagnetic Fields*. New York: McGraw-Hill, 1961.

[9] R. F. Harrington, *Field Computation by Moment Methods*. New York: MacMillan, 1968.

[10] G. Markov, *Antennas*. Moscow: Progress Publishers, 1965.

[11] E. C. Jordan and K. G. Balmain, *Electromagnetic Waves and Radiating Systems*. New Delhi: Prentice-Hall, 1976.


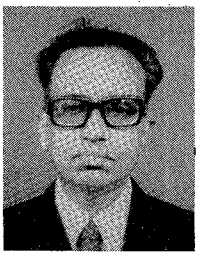

**B. N. Das** received the M.Sc. (Tech.) degree from the Institute of Radio Physics and Electronics, University of Calcutta, India, in 1956. He received the Ph.D. degree in electronics and electrical communication engineering from the Indian Institute of Technology, Kharagpur, in 1967.

He joined the Faculty of the Department of Electronics and Electrical Communication Engineering at Indian Institute of Technology, Kharagpur, in 1958. At present, he is a Professor in the department. He has been actively guiding research in the fields of slot arrays, phased arrays, striplines, and microstrip lines.

Dr. Das has published a large number of research papers in journals in the U.S., U.K., U.S.S.R., and India. His current research interests are electromagnetics, microwave networks, antenna pattern synthesis, printed antennas and EMI/EMC studies. Dr. Das is a Fellow of the Institute of Engineers (India), the Indian National Science Academy, and the Indian National Academy of Engineering.

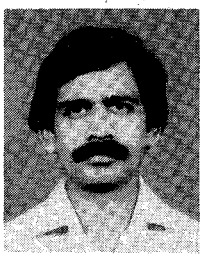

**P. V. D. Somasekhar Rao** received the B.E. degree in electronics and communication engineering from Sri Venkateswara University, Tirupati, India, in 1977 and the M.Tech. degree in microwave and radar engineering from the Indian Institute of Technology, Kharagpur, in 1979.

He was a Senior Research Assistant in the Radar Centre, Indian Institute of Technology, Kharagpur, until May 1980, and was with the Radio Astronomy Centre Group of the Tata Institute of Fundamental Research, Ootacamund, India, as Electronics Engineer until January 1981. Since then he has been on the Faculty of the Department of Electronics and Communication Engineering, Jawaharlal Nehru Technology University, Hyderabad, India. Currently he is with the Department of Electronics and Communication Engineering, Indian Institute of Technology, Kharagpur, where he is working toward the Ph.D. degree under the QIP program.

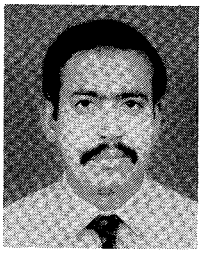

**Ajoy Chakraborty** was born on December 25, 1952. He received the B.Tech., M.Tech., and Ph.D. degrees from the Indian Institute of Technology, Kharagpur, in 1975, 1977, and 1982, respectively.

He joined the Radar Centre of the Indian Institute of Technology, Kharagpur, in 1977. He became a Lecturer in 1980 and was promoted to Assistant Professor in 1984. Currently he is working as an Assistant Professor in the Department of Electronics and Electrical Communication Engineering at the institute. His current interests include array antenna design, antenna feeds, and numerical modeling of waveguide junctions.